

# Effect of Annealing Atmosphere on the Properties and Performance of V + Mo Codoped TiO<sub>2</sub> Thin Films

Chen W.-F.<sup>\*</sup>, Liu L., Koshy P., and Sorrell C.C.

School of Materials Science and Engineering, UNSW Sydney, NSW 2052, Sydney, Australia

\*corresponding author: Chen W.-F.

e-mail: w.chen@unsw.edu.au

**Abstract** Molybdenum (Mo) and vanadium (V) codoped TiO<sub>2</sub> thin films were deposited by spin coating a sol-gel solution on fused silica substrates, followed by annealing in air or argon at 450°C for 2 h. The effects of varying codopant levels (0.01-1.00 mol% each) on the mineralogical, optical, topographical, and chemical properties of the films as well as their photocatalytic performance were analysed.

The results show that the atmosphere played a key role in the mechanisms of structural and nanostructural development. These depended upon codopant solubilities within and beyond the saturation limits, associated lattice destabilization and precipitation, change in the Ti<sup>3+</sup> and oxygen vacancy concentrations, grain growth, and eutectic liquid formation. The detection of oxidized valences following reduction conditions and *vice versa* is explained by the process of multivalence charge transfer.

**Keywords:** Codoping, TiO<sub>2</sub> Thin Film, Photocatalysis

## 1. Introduction

TiO<sub>2</sub> is a photocatalyst of technical interest and applicability owing to its chemical stability, thermal stability, non-toxicity, low cost, high redox capacity, and favorable optoelectronic properties [1]. Several factors affect the its photocatalytic properties and these include particle/grain size, amorphous/crystalline nature, dopant type and concentration, charge-compensating defect type and concentration, synthesis method, and surface properties [2]. Recently, experimental surface reconstruction of pure TiO<sub>2</sub> by treatment under various atmospheres has been attempted [3] in order to enhance the surface defects, particularly oxygen vacancies for increased photocatalytic activity. However, there appears to be no reports on the effects of annealing atmosphere on the photocatalytic performance of codoped TiO<sub>2</sub>.

The present work reports the effects of annealing atmospheres [oxidizing (air) or reducing (argon) conditions] on the photocatalytic performance of TiO<sub>2</sub> thin films codoped with varying molybdenum and vanadium levels. The Mo + V codoped films were produced by spin coating Ti-based precursor solutions on fused silica substrates, followed by annealing in air or argon for 2 h at 450°C. A range of analytical methods was used to characterize the mineralogical, morphological, chemical, and photocatalytic properties of these films.

## 2. Experimental Procedure

### 2.1. Precursor Solution Preparation

Titanium tetra-isopropoxide (TTIP, 97 wt%, Reagent Grade, Sigma-Aldrich) was the Ti precursor solute, while isopropanol (IP, 99 wt%, Reagent Grade, Sigma-Aldrich) was the solvent. The precursor solutions were produced by mixing 5.68 g of TTIP with 200 mL IP in a Pyrex beaker. The identical Mo and V dopant levels were 0.00, 0.01, 0.05, 0.10, 0.50, and 1.00 mol%. The dopant salts were MoCl<sub>5</sub> (Mo<sup>5+</sup>) and VCl<sub>3</sub> (V<sup>3+</sup>) (both ≥99 wt%, Sigma-Aldrich). These were added as solids to the precursor solutions. Each solution was stirred manually at room temperature for 10 minutes in air to ensure complete dissolution.

### 2.2. Thin Film Preparation

The substrates used were fused SiO<sub>2</sub> (99.9% purity, Sunray Oil, Singapore, 20 x 20 x 1 mm<sup>3</sup>). TiO<sub>2</sub> thin films were deposited by spin coating (Laurell WS-65052). During this process, 0.2 mL of solution were deposited on the substrates spun at 2000 rpm in N<sub>2</sub>; each film was dried for 15 s by further spinning; these steps were repeated six more times to obtain films with near-identical thicknesses. The deposited films then were annealed either in a muffle furnace in air or a tube furnace in argon at 450°C for 2 h. The heating rates were 0.5°C/min (25°-200°C) and 1°C/min (200°-450°C); cooling to room temperature was at 1°C/min.

### 2.3. Characterization

The mineralogical properties were determined by glancing angle X-ray diffraction (GAXRD, PANalytical Empyrean X-ray diffractometer, 45 kV, 40 mA). The optical properties were analyzed using ultraviolet-visible spectrophotometry (UV-Vis, PerkinElmer Lambda 35 UV-Visible Spectrometer, dual-beam, aperture 20 mm x 10 mm). The film topographies were assessed by atomic force microscopy (AFM, Bruker Dimension Icon Scanning Probe Microscope, tapping mode, scan size 1 μm x 1 μm). The grain sizes were assessed by the measurement of ten random grains. The surface roughnesses were calculated by the instrument. The surface compositions were analyzed by X-ray photoelectron spectroscopy (XPS, Thermo Scientific ESCALAB 250Xi X-ray Photoelectron Spectrometer Microprobe, 13 kV, 12 mA, spot size 500 μm). The photocatalytic activities were analyzed by photobleaching using UV radiation and exposure of

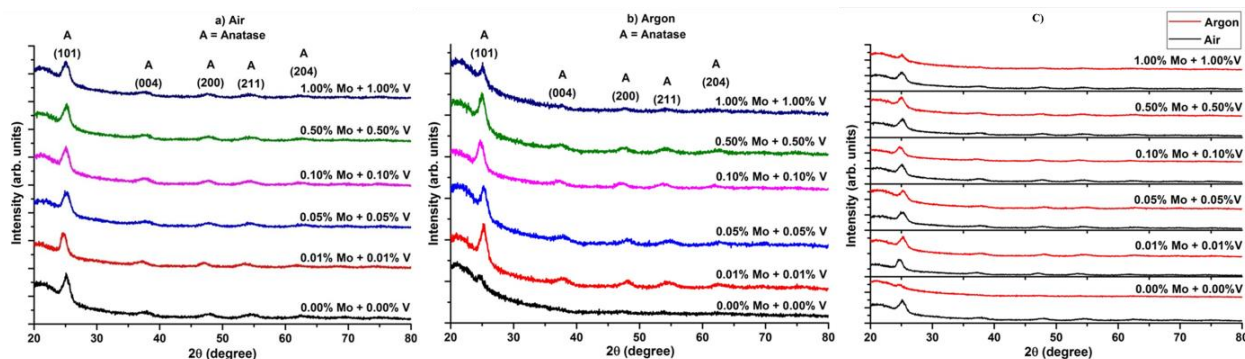


**Figure 1.** XRD patterns of undoped  $\text{TiO}_2$  and Mo + V codoped  $\text{TiO}_2$  thin films after annealing for 2 h at  $450^\circ\text{C}$ : (a) in air, (b) in argon, and (c) comparatively.

methylene blue (MB, M9140, dye content  $\geq 82$  wt%, Sigma-Aldrich) solutions ( $10^{-5}$  M). The films were placed in beakers filled with MB solution and stored for  $\sim 12$  h in a light-obstructing container to ensure complete MB adsorption on the film surfaces. These then were exposed to UV (UVP, 3UV-38, 8 W, lamp-to-film distance 10 cm) for 0-24 h, with the degradation analyzed using UV-Vis spectrophotometry (664 nm).

### 3. Results and Discussion

The GAXRD patterns of undoped  $\text{TiO}_2$  and Mo + V codoped  $\text{TiO}_2$  thin films with different dopant levels after annealing in air or argon for 2 h at  $450^\circ\text{C}$  are shown in Figure 1. Anatase was the only phase detected in all of the films. No rutile, brookite, or crystalline phases containing Mo and/or V compounds were observed in the thin films. This could be because either the dopants were incorporated in the lattice or the dopant amounts were lower than the detection limit of the instrument [4].

Figures 1(a) and 1(b) show that the intensities of the major anatase peak (101) of the  $\text{TiO}_2$  films annealed in air and argon, respectively. Figure 1(a) shows that codoping caused a slight decrease in intensity relative to the undoped sample but that the doping level had little effect. Figure 1(b) shows that codoping caused a significant increase in intensity, followed by a gradual decrease in intensity with increasing codopant level.

For undoped  $\text{TiO}_2$ , these data suggest that oxidation enhances recrystallization and crystallinity relative to reduction. That is, oxidation would increase the  $\text{Ti}^{4+}$  concentration and decrease that of oxygen vacancies while reduction would increase the  $\text{Ti}^{3+}$  concentration and increase that of the oxygen vacancies. These defects are known to cause structural destabilisation and consequent decrease in the crystallinity [5].

For codoped  $\text{TiO}_2$  under oxidizing conditions, there was little effect on the intensities as a function of doping level. These data suggest that the solubilities of the codopants are extremely low ( $\leq 0.01$  mol%) and that the data are consistent with the achievement of saturation and precipitation for all codoped samples.

In contrast, for codoped  $\text{TiO}_2$  under reducing conditions, the effect of codoping was a gradual decrease in the extent of crystallinity. These data are consistent with substantially higher solubility limits and associated greater structural destabilization from  $\text{Ti}^{3+}$  and oxygen vacancies with increasing dopant level. However, the significant increase in intensity at the lowest codopant level relative to the undoped sample indicates that the presence of a low concentration of structural defects in the form of the dopants enhanced the recrystallization of anatase.

Since the solubility limits of the codopants are unknown, the AFM data, discussed subsequently, provide some clarification of the potential for resultant liquid (eutectic) formation. That is, liquid precipitated on the grain boundaries potentially can hinder (or enhance) recrystallization and grain growth, thereby causing a decline in GAXRD peak intensities.

An alternative interpretation is that charge compensation does not occur through oxygen vacancy formation but by intervalence charge transfer (IVCT) [6]. That is redox effects in Ti are compensated by V and/or Mo. This will be discussed subsequently.

The optical transmission spectra and the band gap data are shown in Figure 2. The transmittances of the oxidized films (Figure 2(a)) were  $\sim 80\%$  while those for the reduced films (Figure 2(b)) were  $\sim 60$ - $80\%$ , which is consistent with the differences in crystallinity. It also may be a result of light scattering from recrystallized liquid. If so, reduction should be associated with higher liquid levels. For codoped  $\text{TiO}_2$  under oxidizing conditions, all films showed a slight red shift. The optical indirect band gap of 3.35 eV in parenthesis is considered to be an outlier, which is based on the AFM data discussed subsequently. Previous work by the authors [6] has revealed that V causes a slight red shift in  $\text{TiO}_2$  films deposited on soda-lime silica.

For codoped  $\text{TiO}_2$  under reducing conditions, all films showed a slight blue shift. Again, the optical indirect band gap of 3.40 eV in parenthesis is considered to be an outlier, which is based on the AFM data discussed subsequently. Previous work by other authors [7] reported that Mo results in a significant blue shift in  $\text{TiO}_2$  films deposited on fused silica.

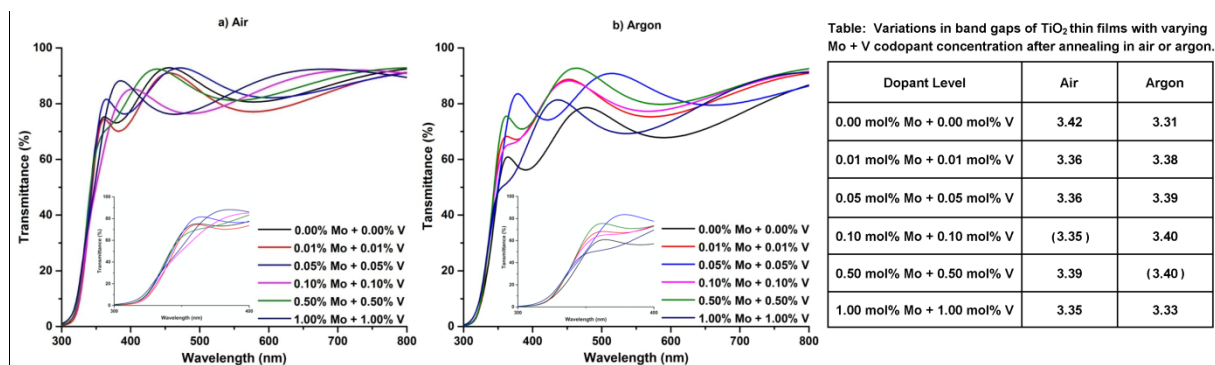


**Figure 2.** UV-Vis transmission spectra of undoped TiO<sub>2</sub> and Mo + V codoped TiO<sub>2</sub> thin films after annealing for 2 h at 450°C: (a) in air, (b) in argon (band gap data are given in adjacent table).

In both cases, Si contamination is believed to have little or no effect since (a) substitutional solid solubility by Si<sup>4+</sup> would not alter the defect chemistry and (2) prior work on Si<sup>4+</sup> contamination from glass substrates suggests that it plays no role [6].

The band gaps calculated by the Tauc method [8] are summarized in Figure 2. The data show that band gap ( $E_g$ ) of the oxidized undoped TiO<sub>2</sub> film (~3.42 eV) was higher than that of the reduced undoped TiO<sub>2</sub> film (~3.31 eV). The differences between the codoped samples are inconsistent, so no conclusion is made. The lower  $E_g$  of the reduced film can be interpreted in terms of the intrinsic effects of the (a) presence of Ti<sup>3+</sup> and oxygen vacancies [6] and (b) lattice distortion from IVCT [6]. Further, the  $E_g$  data can be considered in terms of the extrinsic effects of exceeding of the solubility limit of one or both dopants, precipitation, and decrease in band gap, which is an artefact of the microstructure from reflection [6,9].

Figure 3(a) shows AFM images of films annealed in air. These show that liquid formation, indicated by the uneven topography, probably was limited to only the highest dopant level, although 0.05 mol% Mo + 0.05 mol% V also suggests liquid formation. The film 0.10 mol% Mo + 0.10 mol% V is considered to be an outlier owing to its distinctly different nanostructure.

Figure 3(b) shows AFM images of the films annealed in argon. These data show a considerably greater extent of liquid formation. The film 0.50 mol% Mo + 0.50 mol% V

is considered to be an outlier again owing to its distinctly different nanostructure.

It also may be seen that the grain sizes of the oxidized films tend to be greater than those of the reduced films. This is attributed to the enhanced recrystallization, crystallinity, and grain growth exhibited by the former. Thus, it can be concluded that defects in the form of Ti<sup>3+</sup> and probably oxygen vacancies do not assist recrystallization.

The initial grain size increase with increasing codopant level in the reduced films is consistent with the enhancement of grain growth from the well-known effect of increased fluxing of oxides under reducing atmospheres [6]. This indicates the important role of the Ti<sup>3+</sup> concentration (and possibly that of the oxygen vacancies) in the process.

However, at the highest codopant level, the decrease in grain size is likely to have resulted from exceeding the solubility limit, precipitation, and eutectic liquid formation. This decrease in grain size suggests that the amount of liquid was such that the length of the diffusion path increased to the extent that it dominated the diffusion. This conclusion is supported by the observation that this film had a considerably lower surface roughness than all of the other films, which suggests the formation of a high amount of liquid.

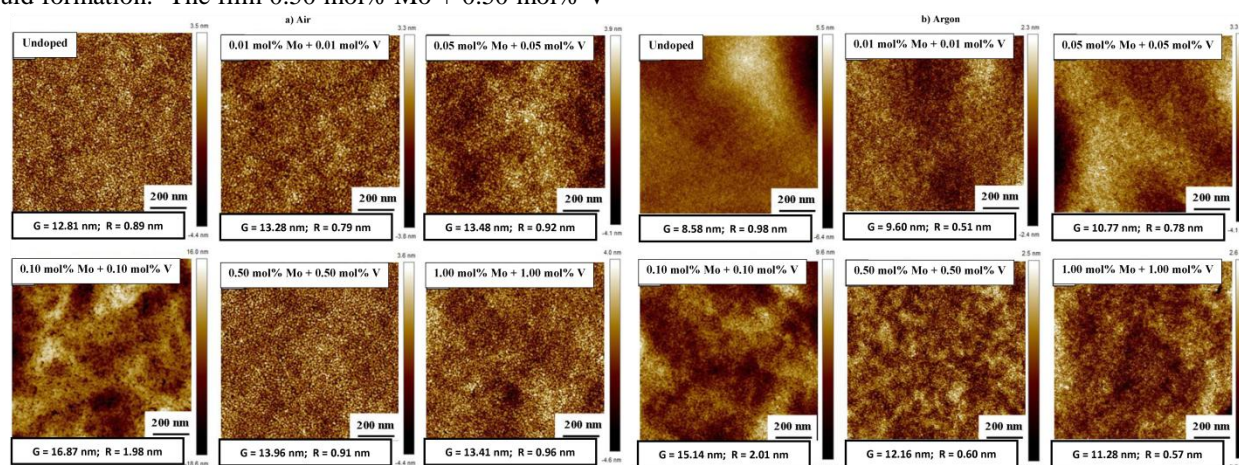


**Figure 3.** AFM topographical images of undoped TiO<sub>2</sub> and Mo + V codoped TiO<sub>2</sub> thin films after annealing for 2 h at 450°C: (a) in air, (b) in argon (G = grain size, R= surface roughness).

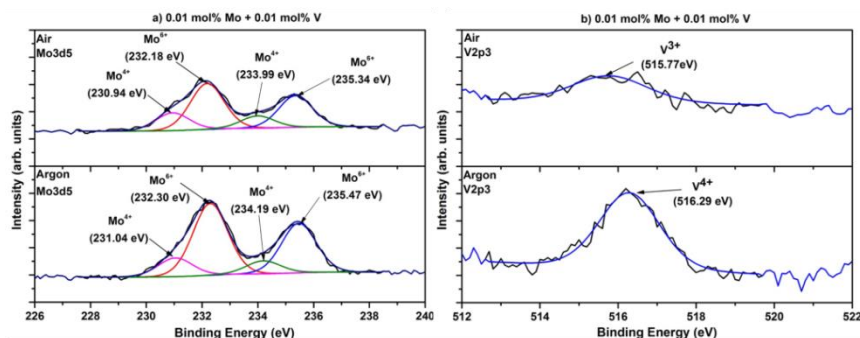


**Figure 4.** XPS spectra of 0.01 mol% Mo + 0.01 mol% V codoped TiO<sub>2</sub> thin films after annealing in air and argon for 2 h at 450°C: (a) Mo3d5, (b) V2p3 regions.

The XPS data in Figure 4(a) show that both types of samples exhibited the same Mo species. However, the Mo<sup>6+</sup> peak intensities were lower for the oxidized film relative to that of the reduced film while the Mo<sup>4+</sup> peak intensities were constant. The difference in the Mo<sup>6+</sup> peaks is a paradox since oxidation would be expected to increase these intensities but had the opposite effect. The XPS data in Figure 4(b) show that peak intensities for the V species exhibit the same paradoxical behavior, where the oxidized valence was generated during reduction and *vice versa*. Here, this is even clearer since only a single valence was detected for each redox condition. These data can be explained by IVCT or, more specifically, multivalence charge transfer (MVCT), in which charge transfer occurs between multiple dopant cations as well as the lattice cation [10]. As shown in the summary of these effects in Figure 5, the observation of Mo<sup>6+</sup> and Mo<sup>4+</sup> in both oxidized and reduced films supports the conclusion, which cannot be confirmed by XPS owing to peak overlaps, that Ti<sup>4+</sup> ↔ Ti<sup>3+</sup> charge transfer has occurred. The analytical techniques used to assess the presence of the specific ions also are given.

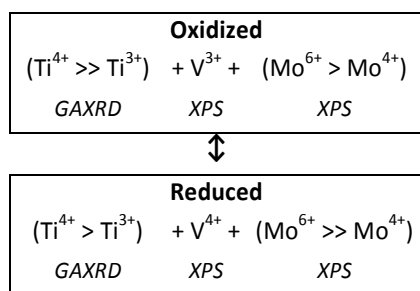


**Figure 5.** Proposed redox equilibria resulting from MVCT, with validating experimental data.

Figure 6(a) shows the photocatalytic performances of the films in terms of MB degradation under UV irradiation for both redox conditions.

For the oxidized films, the 0.01 mol% Mo + 0.01 mol% V film showed the best performance. This is considered to occur because the TiO<sub>2</sub> was at or near the solubility limits of the codopants, thus yielding a homogeneous film doped at a semiconducting level [6]. Higher dopant levels (the outlier is in parenthesis) resulted in a slight increase in performance. Since the crystallinity, E<sub>g</sub>, and grain size data indicate no significant differences between these samples, this result is attributed to precipitation and the gradual coverage of the photocatalytically active sites by these precipitates.

For the reduced films, the 0.01 mol% Mo + 0.01 mol% V film also showed the best performance for the same reason [6]. The decrease in photocatalytic activity at the highest codopant level is attributed to the recrystallization of the eutectic liquid and consequent greater blockage of the active sites. If the data for the intermediate dopant levels are accurate (the outlier is in parenthesis), then these data show a trend opposite to that of the oxidized samples. Since the performance appears to increase with increasing dopant level, this is not consistent with the decreasing crystallinity or lattice destabilization. However, while the E<sub>g</sub> data are inconclusive, the grain size data show a consistent trend in that the performance increases with increasing grain size. This effect has been observed by the authors previously for thin films comprised of spherical grains,

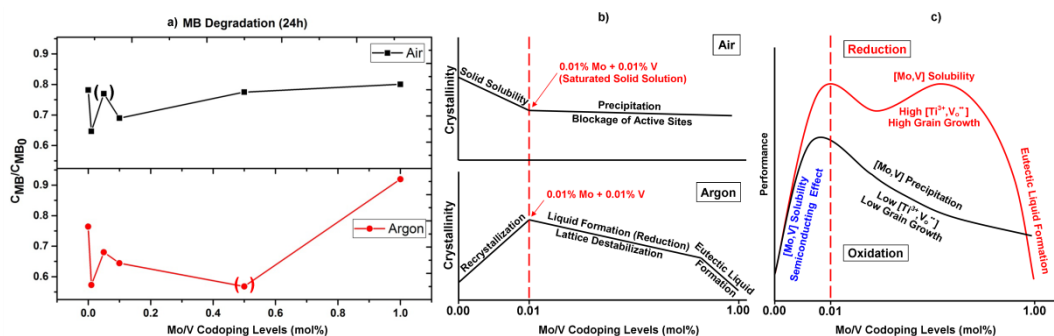


**Figure 6.** Photodegradation rates of undoped and Mo + V codoped TiO<sub>2</sub> thin films after annealing for 2 h at 450°C: (a) comparison, (b) mechanisms (crystallinity), (c) mechanisms (photocatalytic performance).

where the effect is a reflection of the surface area only, which is independent of the grain volume [11].

#### 4. Summary

Figure 4(b) illustrates structural and nanostructural mechanisms in terms of crystallinity and codopant level. Figure 4(c) illustrates these mechanisms in terms of their effects on the performance.

For the oxidized films, the lowest codopant level was in the semiconducting range, so the effect of the codopants in the homogeneous lattice was an increase in performance. At higher codopant levels, the solubility limit was exceeded and so any lattice distortion remained constant, did not contribute to lattice destabilization, and hence did not contribute to a decrease in the photocatalytic performance. Likewise, the crystallinity remained constant. The slight red shift would have been expected to improve the performance, so the  $E_g$  is not a key factor in the performance. However, the gradually increasing precipitation resulted in greater blockage of the active sites and hence resulted in a decrease in the photocatalytic performance. The oxidizing atmosphere favored the presence of  $Ti^{4+}$  and hence minimized the  $Ti^{3+}$  and oxygen vacancy concentrations. The absence of these defects did not assist recrystallization or grain growth and the concentrations of these structural defects were reduced. In effect, the low photocatalytic performances can be attributed to (a) blockage of the active sites by the precipitates, (b) low concentrations of  $Ti^{3+}$  and oxygen vacancies, and (c) low surface areas on small grains.

For the reduced films, again, the lowest codopant level was in the semiconducting range and so there was an increase in performance. At the same time, the presence of the codopants enhanced recrystallization and lattice perfection, thereby providing a second cause for the increased performance. At higher codopant levels, the greater solubilities of the codopants resulted in the contribution of several concurrent effects. (a) Reduction facilitated the  $Ti^{3+}$  and oxygen vacancy concentrations, which would be expected to increase the performance. (b) However, increasing codopant concentrations would be expected to destabilize the lattice and so decrease the performance. (c) The increasing grain size from liquid formation from reduction would be expected to increase the performance. (d) At the highest codopant level, the formation of a eutectic liquid resulted in an excessive amount of liquid formation, which reduced grain growth and blocked the active sites, both of which would be expected to decrease the performance. The dominance of one or more of these four factors can explain the variable performances as a function of codopant level.

Examination of the combined GAXRD and XPS data indicates that the explanation for the paradoxical observation of oxidized valence states following reduction conditions and *vice versa* can be explained by multivalence charge transfer [10], in which the codopant and lattice cations exchange electrons. This mechanism provides support for the logical conclusion that the  $Ti^{3+}$  concentration increases under reduction, which cannot be confirmed by XPS.

#### Acknowledgements

The authors acknowledge the financial support from the Australian Research Council (ARC) and the

characterisation facilities provided by the Australian Microscopy & Microanalysis Research Facilities (AMMRF) node at UNSW Sydney.

#### References

- [1] Schneider J., Matsuoka M., Takeuchi M., Zhang J., Horiuchi Y., Anpo M., and Bahnemann D.W. (2014), Understanding  $TiO_2$  photocatalysis: mechanisms and materials, *Chemical Reviews*, **114**, 9919-9986.
- [2] Plugaru R., Cremades A., and Piqueras J. (2003), The effect of annealing in different atmospheres on the luminescence of polycrystalline  $TiO_2$ , *Journal of Physics: Condensed Matter*, **16**, S261-S268.
- [3] Asari E. and Souda R. (2002), A study of reactivity of  $O_2$  gas on the  $TiO_2$  (110) surface: low and heavily reduced surfaces, *Vacuum*, **68**, 123-129.
- [4] Wu, J.C.S. and Chen C.H. (2004), A visible-light response vanadium-doped titania nanocatalyst by sol-gel method, *Journal of Photochemistry and Photobiology A: Chemistry*, **163**, 509-515.
- [5] Estrellan C.R., Salim C., and Hinode H. (2009), Photocatalytic activity of sol-gel derived  $TiO_2$  co-doped with iron and niobium. *Reaction Kinetics and Catalysis Letters*, **98**, 187-192.
- [6] Chen W.-F., Koshy P., Huang Y., Adabifiroozjaei E., Yao Y., and Sorrell C.C. (2016), Effects of precipitation, liquid formation, and intervalence charge transfer on the properties and photocatalytic performance of cobalt- or vanadium-doped  $TiO_2$  thin films. *International Journal of Hydrogen Energy*, **41**, 19025-19056.
- [7] Hagberg D.P., Edvinsson T., Marinado T., Boschloo G., Hagfeldt A. and Sun L. (2006), A novel organic chromophore for dye-sensitized nanostructured solar cells, *Chemical Communications*, **21**, 2245-2247.
- [8] Tauc J. and Menth A. (1972), States in the gap. *Journal of Non-Crystalline Solids*, **8**, 569-585.
- [9] Kay A. and Graetzel M. (1993), Artificial photosynthesis. I. Photosensitization of titania solar cells with chlorophyll derivatives and related natural porphyrins, *The Journal of Physical Chemistry*, **97**, 6272-6277.
- [10] Ren, H., Koshy, P., Chen, W.-F., Qi, S. and Sorrell, C.C. (2017), Photocatalytic materials and technologies for air purification, *Journal of Hazardous Materials*, **325**, 340-366.
- [11] Chen, W.-F., Koshy, P. and Sorrell, C.C. (2016), Effects of film topology and contamination as a function of thickness on the photo-induced hydrophilicity of transparent  $TiO_2$  thin films deposited on glass substrates by spin coating, *Journal of Materials Science*, **51**, 2465-2480